Tellus SERIES B CHEMICAL AND PHYSICAL METEOROLOGY
PUBLISHED BY THE INTERNATIONAL METEOROLOGICAL INSTITUTE IN STOCKHOLM

Evaluating aerosol direct radiative effects on global terrestrial ecosystem carbon dynamics from 2003 to 2010

By MIN CHEN[1,2]* and QIANLAI ZHUANG[1,3], [1]*Department of Earth, Atmospheric, and Planetary Sciences, Purdue University, West Lafayette, IN, USA;* [2]*Department of Organismic and Evolutionary Biology, Harvard University, Cambridge, MA, USA;* [3]*Department of Agronomy, Purdue University, West Lafayette, IN, USA*

(Manuscript received 20 June 2013; in final form 24 April 2014)

ABSTRACT

An integrated terrestrial ecosystem model and an atmospheric radiative transfer module are developed and applied to evaluate aerosol direct radiative effects on carbon dynamics of global terrestrial ecosystems during 2003–2010. The Moderate-Resolution Imaging Spectroradiometer measurements of key atmosphere parameters have been used to quantify aerosol effects on downward solar radiation. Simulations with and without considering the aerosol loadings show that aerosol affects terrestrial ecosystem carbon dynamics through the effects on plant phenology, thermal and hydrological conditions as well as solar radiation. The simulations also show that aerosol enhances the terrestrial gross primary production by 4.9 Pg C yr^{-1}, the net primary production by 3.8 Pg C yr^{-1}, the net ecosystem production by 3.9 Pg C yr^{-1}, and the plant respiration by 1.1 Pg C yr^{-1} during the period. The aerosol loading at a magnitude of 0.1 Pg C $yr^{-}1$ reduces ecosystem heterotrophic respiration. These results support previous findings of the positive effects of aerosol light scattering on plant production, but suggest there is a strong spatial variation due to cloud cover. This study suggests that both direct and indirect aerosol radiative effects through aerosol–cloud interactions should be considered to quantify the global carbon cycle.

Keywords: aerosol, carbon dynamics, terrestrial ecosystem model

1. Introduction

Atmospheric aerosol has been considered to be able to scatter and reduce the total of downward solar radiation, but enhance the diffusive fraction (Mahowald et al., 2011b), which is referred to as the aerosol direct radiative effect. Micrometeorological environment in the land surface is therefore influenced by the aerosol-induced change of downward solar radiation regime. Multiple studies have suggested that the aerosol direct radiative effect has considerable impacts on terrestrial plant productivity and carbon budgets (Roderick et al., 2001; Gu et al., 2003; Krakauer and Randerson, 2003; Niyogi et al., 2004; Oliveira et al., 2007).

The impact of aerosol on terrestrial carbon sink could be either positive or negative. Because of the strong light-scattering effect, the aerosol loading normally induces lower solar energy arriving at the land surface whereas plant photosynthesis tends to decrease with weakening surface irradiance. The positive effect lies in the advantage of diffuse solar radiation for plant carbon uptake. Comparing with direct-beam solar radiation, diffuse solar radiation can be more homogeneously absorbed by plant canopy and more efficiently used for photosynthesis without the occurrence of photosynthetic saturation. In contrast, direct-beam radiation can only be absorbed by a sunlit canopy in which photosynthesis is often light-saturated. Roderick et al. (2001) conducted a theoretical analysis of the radiation–photosynthesis relationship and emphasised the importance of diffuse radiation fraction on canopy photosynthesis. They further indicated that the eruption of the Mount Pinatubo might increase plant productivity by the light scattering effect of the erupted aerosols. Gu et al. (2003) reported an observed increased plant carbon uptake after the massive volcano eruption of the Mount Pinatubo at a deciduous

*Corresponding author.
email: minchen@fas.harvard.edu

Citation: Tellus B 2014, **66**, 21808, http://dx.doi.org/10.3402/tellusb.v66.21808

forest site in North America. In contrast, Krakauer and Randerson (2003) found that plant productivity decreased in the boreal regions after the eruption of Mount Pinatubo probably because of aerosol-driven temperature feedbacks. Several other studies have suggested that both positive and negative impacts of aerosol could happen on ecosystem carbon uptake depending on the amount of aerosol loading, cloud cover, canopy structure and other environmental conditions. For example, by investigating the effect of biomass-burning-derived aerosols on the terrestrial carbon sink over the Amazon basin during the dry season, Oliveira et al. (2007) found that forest productivity was enhanced under the moderately thick smoke loading because of an increase of diffuse solar radiation; their results also indicated that large aerosol loading [i.e. the Aerosol Optical Depth (AOD) >2.7] can result in lower net productivity of the Amazon forest. Cohan et al. (2002) quantified the change in plant net primary production (NPP) caused by aerosol alteration of direct-beam and diffuse radiation and concluded that the aerosol effect could be positive, neutral or negative depending on the AOD values and cloud cover fractions. By analysing the AOD, diffuse radiation and carbon fluxes observed over widely distributed sites over different terrestrial ecosystems, Niyogi et al. (2004) found that high AOD with clear sky may increase daytime carbon sink for forests and croplands but a negative effect on grassland, and suggested that canopy structure could be an important factor of the direction of the aerosol effect.

The change of surface solar radiation regime caused by aerosol could potentially alter the energy partitioning and the environmental conditions such as land surface temperature, and therefore the water cycle. Both the effects of changing thermal and moist conditions are not negligible while examining the aerosol direct radiative effect on terrestrial ecosystem carbon dynamics. Given the considerable spatial and temporal variations of aerosol loading amount, meteorological forcing, the environmental states and the plant functional types in large areas, more adequately estimating the aerosol direct radiative effect on carbon dynamics is needed by simultaneously considering the aerosol effect on radiation regime, thermal condition and hydrological condition. To date, there are few studies focusing on examining the aerosol direct radiative effect at large spatial scales. Matsui et al. (2008) used a regional land surface model to conduct simulations of surface carbon fluxes and energy fluxes to examine the effect over the eastern United States for the growing seasons in 2000 and 2001. The study suggested that the aerosol effect could vary due to different leaf area index (LAI) of surface vegetation, AOD and cloud optical depth (COD) by examining deeply into the detailed biogeochemical processes in sunlit and shaded leaves. These conclusions are useful for better understanding the aerosol effect, but the study's short period and small region cannot present a view of the global pattern of aerosol effects, which may have a considerable spatial heterogeneity due to different climate patterns and land cover. Mercado et al. (2009) utilised the land surface model, the Joint UK Land Environment Simulator (JULES), to examine the change of global carbon sink after the eruption of Mount Pinatubo in 1992 and 1993, and found both abnormally low air temperatures and enhanced carbon sinks due to the contribution of diffuse radiation. Their study examined both plant carbon uptake and ecosystem respiration at the global scale under the changing radiation regimes with the aerosol loadings, but lacking detailed mechanistic information of the aerosol effect. Furthermore, the study reconstructed the shortwave solar radiation using global climate dataset [i.e. the Climatic Research Unit (CRU) data], which is deviated from ground observations. Coupled-carbon–climate studies by Mahowald et al. (2011a) pointed out that the aerosols could significantly impact regional climate and biogeochemistry, but not significantly impact the globally averaged carbon cycle. However, their study may underestimate the aerosols' effect on the global carbon cycle, since the terrestrial biosphere model they used is the Community Land Model–Carbon Nitrogen (CLM–CN), which has not well simulated the thermal and hydrological dynamics separately for sunlit and sunshade leaves, while both theoretical and observational studies suggest these dynamics are important to plant photosynthesis.

It is important to have both accurate estimations of radiation and a realistic modelling framework of coupled land-surface biophysical and biogeochemical processes to evaluate the aerosol direct radiative effect on terrestrial ecosystem carbon dynamics. Here we present a study that aims to better understand the aerosol direct radiative effect on terrestrial ecosystem carbon dynamics at the global scale. Atmosphere profile parameters such as cloud fraction (CF) and optical depth, AOD, water vapour amount and ozone column amount are critical for atmosphere radiative transfer models to estimate downward solar radiation and its partitioning. These parameters are available globally through satellite measurements [e.g. the Moderate-Resolution Imaging Spectroradiometer (MODIS)], which are considered to be more accurate and have higher spatial resolution compared to Global Climate Model (GCM) estimates. In addition, a coupled ecosystem model, the integrated Terrestrial ecosystem model (iTem), has also been developed to simulate biophysical processes in both sunlit and shaded leaves and the nutrient feedback to carbon dynamics.

Below, we first introduce the modelling framework including the atmospheric radiative transfer module and the iTem. We then describe the data used in this study and the design of model simulations. Finally, we discuss aerosol effects on the land-surface biophysical and biogeochemical

processes, in turn, carbon dynamics of the terrestrial ecosystems at the global scale.

2. Modelling framework

The modelling framework includes two components: (1) the atmospheric radiative transfer module, providing the estimation of solar radiation components (i.e. the direct-beam and diffusive radiation in the visible and near infrared bands) and (2) the terrestrial ecosystem module, representing the land-surface biophysical and biogeochemical processes.

2.1. Atmospheric radiative transfer module

We use an atmospheric radiative transfer module that combines a clear-sky solar radiation model and a cloud transmittance algorithm to estimate incident downward solar radiation over the land surface under all-sky conditions. The clear-sky model, Reference Evaluation of Solar Transmittance, 2 bands (REST2), is a two-broadband model that covers the visible and near-infrared bands and has been well parameterised and validated (Gueymard, 2008, 2012). REST2 is designed in a simple radiative-transfer manner to estimate both direct beam and diffuse radiation under cloudless conditions, which are calculated as functions of individual transmittance and scattering coefficients of major atmospheric constituents including well-mixed gases, ozone, nitrogen dioxide, water vapour and aerosols. It considers the scattering or absorbing processes of key atmospheric components including aerosols, clouds, ozone and water vapour and air molecules. The REST2 is optimised and validated with observed direct and diffused solar radiation data. The estimated diffuse solar radiation excludes the strong forward-peak aerosol-scattered radiation by matching the modelled data with the observations. The two-stream approximation method developed by Stephens et al. (1984) is then used to calculate cloud reflectance and transmittance for incident solar radiation by assuming cloud is a single-plane homogeneous layer. An additional d-function adjustment is applied to cloud optical thickness and single scattering albedo to incorporate the forward peak contribution to the direct-beam radiation in multiple scattering processes (Liou, 2002). MODIS atmosphere products continuously provide instantaneous measurements of global atmospheric profile parameters that are needed in our computing scheme. The level-3 product (MOD08 for 8-d and monthly) has been released for global application purposes, which is averaged at a one-degree spatial resolution and contains all of the related atmospheric parameters. We use the daily product since aerosol lifetime is normally shorter than a week (Shekar Reddy and Venkataraman, 2000). The validation at observational sites all over the world shows that the model-estimated direct-beam and diffuse solar radiation are more accurate than the large-scale reanalysis data and have a good agreement with the observed data of the Baseline Surface Radiation Network (BSRN) (Chen, 2013).

2.2. Terrestrial ecosystem module

We use a ecosystem model, the iTem (Chen, 2013), to simulate land surface processes and the terrestrial ecosystem carbon dynamics responding to aerosol direct radiative effects. The structure of iTem combines the advantage of the Land Surface Model 1.0 (Bonan, 1996), the Terrestrial Ecosystem Model (TEM) (Raich et al., 1991; McGuire et al., 1992, 1993; Zhuang et al., 2003; Lu and Zhuang, 2010; Chen et al., 2011; Chen and Zhuang, 2012; Lu et al., 2013), and incorporates acclimating temperature response of key biogeochemical processes such as photosynthesis and plant respiration (Kattge and Knorr, 2007; Ziehn et al., 2011; Chen and Zhuang, 2013). In iTem, the canopy is particularly modelled in a one-layer, two-big-leaf approach (Dai et al., 2004), which diagnoses energy budget, leaf temperature and photosynthesis separately for sunlit and shaded leaves. The model assumes the foliage has zero heat capacity (Dai et al., 2004). The response of biogeochemical processes such as photosynthesis and leaf respiration to temperature are modelled as functions of the plant growing temperature (i.e. the average daily minimum ambient air temperature in the preceding month) rather than using constant parameters. Prognostic LAI is used to scale up leaf level processes to the canopy level. These algorithms adapted in iTem allow the model to better simulate the response of land surface processes to changing direct-beam and diffuse radiation regime and the potentially caused different energy budget and temperature distribution in canopy, which could considerably influence the processes of carbon dynamics. The incorporation of the Carbon–Nitrogen interaction mechanisms originally from TEM enables the iTem to simulate the Nitrogen limitation effects on carbon-related processes (McGuire et al., 1992). The iTem has been calibrated using various sources of observation data. Technical details of the iTem are documented in Chen (2013).

3. Modelling experiment design and the input data

Using the iTem, two sets of model simulations are conducted to estimate ecosystem dynamics with and without considering aerosol loadings. The first simulation (referred to as S0) uses transient solar radiation data estimated with the atmospheric radiative transfer model considering the aerosol loadings and other meteorological forcings. The second simulation (S1) uses the atmospheric radiative model

estimated solar radiation data without considering the aerosol loadings, but keeps using the same other meteorological data forcing. The aerosol direct radiative effect therefore can be evaluated by calculating the differences between S0 and S1 simulations and environmental variables (S0–S1). The experiments are designed to examine the offline aerosol–terrestrial feedback, i.e. without including nonlinear feedback of atmospheric circulation. We shorten 'aerosol direct radiative effect' to 'aerosol effect' unless we specify otherwise in this paper.

To analyse the aerosol effects, we use iTem to simulate the following flux variables including the gross primary production (GPP), NPP, the net ecosystem production (NEP), the autotrophic respiration (R_A) and the heterotrophic respiration (R_H). In addition, we also simulated land surface temperature (T_s), leaf temperatures ($T_{l,sun}$ and $T_{l,sha}$) and the carboxylation and electron transport rate in both sunlit and shaded leaves ($J_{C,sun}$, $J_{C,sha}$, $J_{E,sun}$, and $J_{E,sha}$); the first-layer soil temperature (ST1) and water content (SM1) which represent the major controlling factors on carbon cycling processes in the soil. The subscripts 'sun' and 'sha' in the variables represent the variable of sunlit and shaded leaves, respectively.

iTem is run at a $1^\circ \times 1^\circ$ grid resolution for the whole global land area except the Antarctic. The land cover map adapts the potential natural vegetation distribution used in TEM (Melillo et al., 1993) and is upscaled from $0.5^\circ \times 0.5^\circ$ to $1^\circ \times 1^\circ$ resolution by allowing sub-grid plant functional types (PFTs) to exist in each pixel (Fig. 1). The global spatial explicit soil texture data describing the percentage of sand, silt and clay in the soil are from the soil map of Food and Agriculture Organization of the United Nations (FAO/Unesco). Soil colour for each grid cell is from the data used in LSM 1.0 (Bonan, 1996). Surface elevation data is from Melillo et al. (1993). All these auxiliary data are resampled to a $1^\circ \times 1^\circ$ resolution to match the resolution of the land cover data.

Meteorological forcing data including longwave radiation (L), air temperature (T_{gcm}), wind speed (w_{gcm}), specific humidity (q_{gcm}), and atmosphere pressure (P_{gcm}) are from the global meteorological forcing dataset developed by the Land Surface Hydrology Research Group in Princeton University (Sheffield et al., 2006). These meteorological data are gridded to a $1^\circ \times 1^\circ$ resolution and at a 3-hourly time step. Solar radiation data including the direct-beam photosynthetic active radiation (PAR_b), diffuse photosynthetic active radiation (PAR_d), direct-beam near infrared radiation (NIR_b) and diffuse near infrared radiation (NIR_d) are estimated using the atmospheric radiative transfer module and MODIS daily atmosphere products for each $1^\circ \times 1^\circ$ grid cell of the global land area. Both MODIS Terra and Aqua products (MOD08_D3 and MYD08_D3, collection 051) are used to obtain solar radiation. The MODIS Terra observation is assumed to be representative of morning atmospheric conditions, while the MODIS Aqua observation is used for the afternoon atmosphere (Van Laake and Sanchez-Azofeifa, 2005). In addition, White-Sky albedos of global land from the 8-d MCD43C3 products are

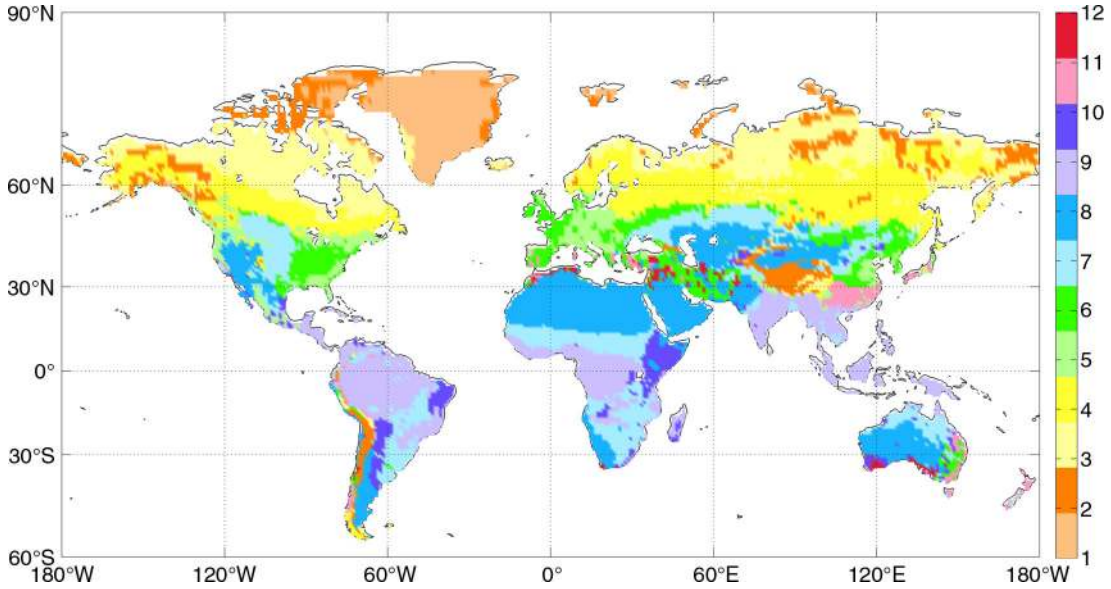

Fig. 1. Global potential natural vegetation map used in this study. The map shown here is the map of the dominant plant functional types in each $1^\circ \times 1^\circ$ grid cell. The labels are: (1) ice; (2) Alpine tundra and polar deserts; (3) wet tundra; (4) boreal forest; (5) temperate coniferous forest; (6) temperate deciduous forest; (7) grasslands; (8) xeric shrublands; (9) tropical forests; (10) xeric woodland; (11) temperate broadleaved evergreen forest; (12) Mediterranean shrublands.

used for calculation of multiple scattering between the sky and land surface. We assume that the land surface albedo remains constant during each 8-d period. Missing values of each parameter are filled using a gap-filling algorithm based on discrete cosine transforms (Garcia, 2010, 2011). The input MODIS parameters are listed in Table 1.

The solar radiation data are estimated at a 3-hourly time step to match the temporal resolution of the meteorological data. Both conditions with and without aerosol loadings are considered to provide two sets of solar radiation data. We use transient atmospheric CO_2 concentration data rather than a constant value. The Mauna Loa monthly mean CO_2 data (http://www.esrl.noaa.gov/gmd/ccgg/trends/) is used with the assumption of no CO_2 concentration change in a month and over the globe. The period of estimation of solar radiation is over the MODIS era (2003–2010). Overlapping the available period of the meteorological forcing data (1948–2010), the model simulations are conducted for the period 2003–2010 at an hourly time step. All the meteorological forcing data are linearly interpolated to an hourly time step.

Driven by monthly NCEP/NCAR reanalysis meteorological data from 1948 to 2002 (Kistler et al., 2001), TEM is run globally to output all C and N state variables and the values of the variables at the end of 2002 (i.e. December of 2002), which are extracted for each $0.5^\circ \times 0.5^\circ$ grid cell. These $0.5^\circ \times 0.5^\circ$ values are then organised as the initial C and N states for each sub-grid PFT in the $1^\circ \times 1^\circ$ grid cells in iTem simulations. In addition, the soil moisture profile is initialised with the 6-hourly soil moisture data (0–10 cm and 10–200 cm) from the NCEP/NCAR reanalysis datasets of the end of 2002 (Kalnay et al., 1996). The surface temperature, vegetation temperature, soil temperature are initialised using air temperature at the beginning of the simulation period.

4. Results

4.1. Aerosol-caused changes of downward solar radiation

The aerosol loading decreases the total and direct downward solar radiation but increases the diffuse component at the global scale. Based on the estimates of the atmospheric radiative transfer module, the existence of aerosols causes 18.7 and 12.8 W m^{-2} decrease of direct-beam PAR and NIR, and 5.2 and 4.4 W m^{-2} increase of diffuse PAR and NIR, respectively, leading to a total 21.9 W m^{-2} decrease of total downward solar radiation over the global land surface. However, the aerosol's effect on solar radiation is spatially heterogeneous (Fig. 2). The aerosol loading generally increased diffuse solar radiation over all the global land area and the magnitude is especially high in the area with high AOD such as East Asia and northern India, and the arid area in Sahara desert area, the Mid-east and Middle Asia.

Table 1. MODIS parameters used in the calculation of downward solar radiation

Data fields	MODIS product name	Descriptions
Total_Ozone_Mean	MOD08_D3/ MYD08_D3	Total ozone column (cm)
Cloud_Top_Pressure_Mean	MOD08_D3/ MYD08_D3	Cloud top pressure (Pa)
Cloud_Optical_Thickness_Combined_Mean	MOD08_D3/ MYD08_D3	Cloud optical thickness
Angstrom_Exponent_Land_Mean	MOD08_D3/ MYD08_D3	Ångström exponent (Land) for 0.47 and 0.66 microns
Deep_Blue_Angstrom_Exponent_Land_Mean	MOD08_D3/ MYD08_D3	Deep Blue Ångström Exponent for land (0.412–0.47 micron)
Angstrom_Exponent_1_Ocean_Mean	MOD08_D3/ MYD08_D3	Ångström Exponent (0.550 and 0.865 micron) best solution
Optical_Depth_Land_And_Ocean_Mean	MOD08_D3/ MYD08_D3	Aerosol Optical Thickness at 0.55 microns for both Ocean and Land
Deep_Blue_Aerosol_Optical_Depth_550_Land_Mean	MOD08_D3/ MYD08_D3	Deep blue aerosol optical depth at 0.55 microns for land
Atmospheric_Water_Vapor_Mean	MOD08_D3/ MYD08_D3	Total perceptible water vapour column (cm)
Cloud_Fraction_Mean	MOD08_D3/ MYD08_D3	Cloud fraction
Albedo_WSA_vis Albedo_WSA_nir	MCD43C3	White-Sky land Albedo for the VIS and NIR broadbands

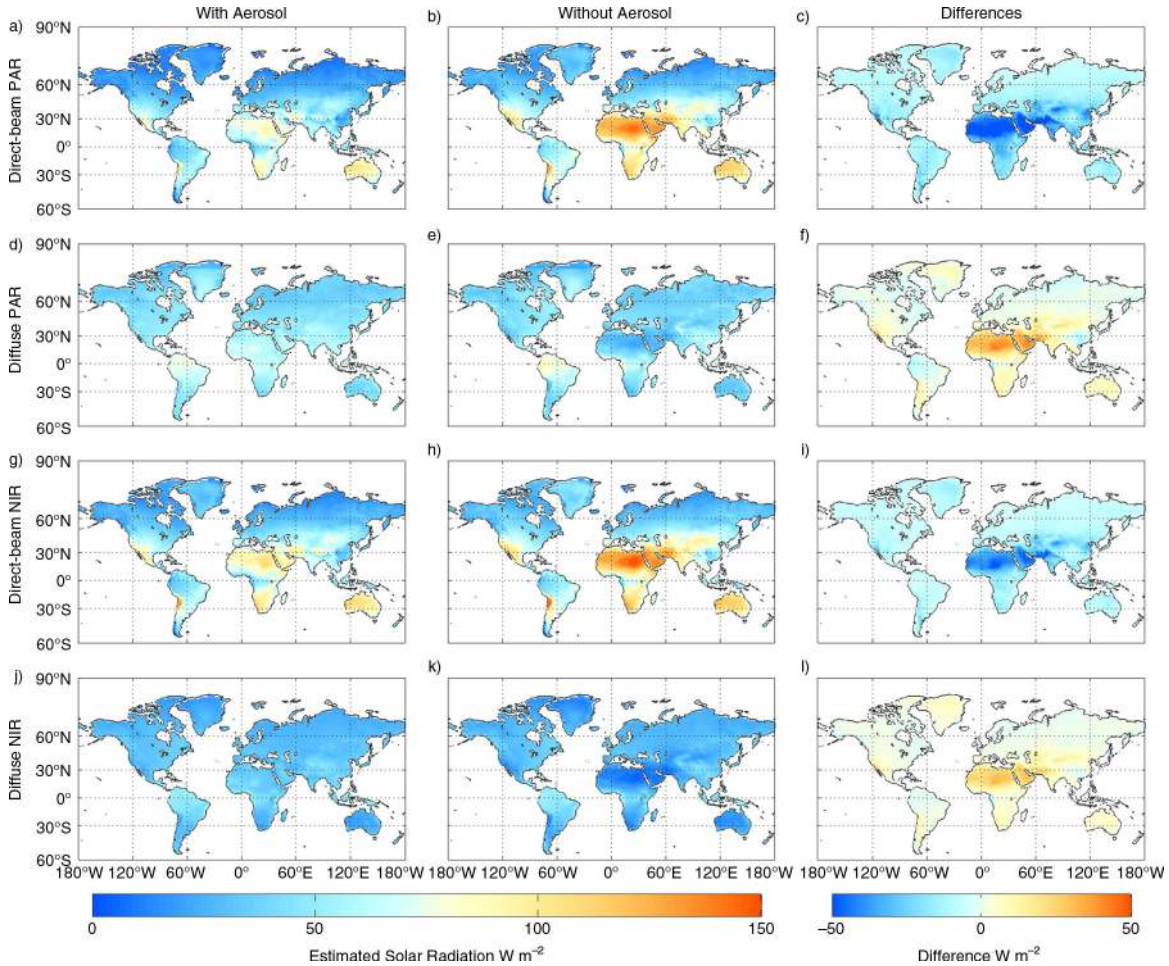

Fig. 2. Annual mean land surface solar radiation of 2003–2010 estimated with or without aerosols and their differences. The difference is calculated as the estimates with aerosols subtract the estimates without aerosols.

Aerosol loading increased diffuse radiation in most terrestrial area, but it decreased the diffuse radiation in Amazonia forest area, forested region in South China, Indonesia Islands and part of the East central Africa.

Two cloud parameters are involved in the calculation of downward solar radiation, including the CF and the COD. The spatial pattern of the estimated global solar radiation indicates that the CF may have a stronger effect than the COD (Fig. 3). Clouds with even small optical depths have much stronger light-scattering effects than aerosols. The regions where aerosol negatively affects diffuse radiation were experiencing either low or high CODs but generally high CFs (Fig. 3). On the one hand, aerosol loading reduced total solar radiation over these regions, which caused less solar radiation above clouds and resulted in reduced direct and diffuse radiation under clouds. On the other hand, aerosols-enhanced diffuse radiation is negligible comparing to the effects of the reduction of cloud on diffuse radiation because of strong cloud scattering, therefore both direct and diffuse solar radiation are reduced over these regions.

4.2. *Global-scale aerosol effects on carbon dynamics*

Over the period of 2003–2010, the S0 estimated GPP, R_A and R_H of global terrestrial ecosystem are 130.0 ± 4.1, 66.5 ± 0.6 and 52.1 ± 1.8 Pg C yr^{-1}, respectively. As a result, NPP and NEP are 63.5 ± 3.6 and 11.4 ± 4.5 Pg C yr^{-1}, respectively. These results are within a reasonable range of existing studies. For example, Yuan et al. (2010) used the EC-LUE model with MODIS land products for the period 2000–2003 and found that global GPP is 110.5 ± 21.3 Pg C yr^{-1}. Cramer et al. (1999) suggested that global NPP ranges from 39.9 to 80 Pg C yr^{-1} using 16 global ecosystem models. The R_A, R_H and NEP values are close to the values reported by the Intergovernmental Panel on Climate Change (IPCC) report as about 60, 50 and 10 Pg C yr^{-1}, respectively (IPCC, 2000). However, S1 estimates lower GPP, NPP, NEP and

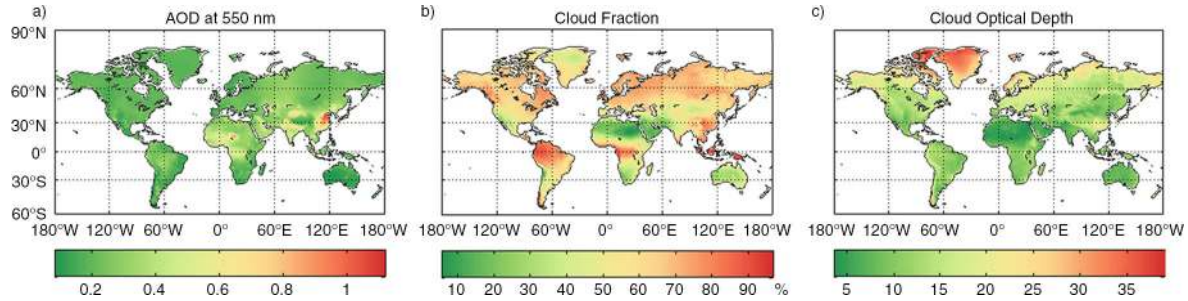

Fig. 3. Gap-filled 2003–2010 mean values of MODIS AOD, COD and cloud fraction over the global land area.

R_A, which are 125.1 ± 5.2, 59.7 ± 4.3, 7.5 ± 4.7 and 65.4 ± 1.0 Pg C yr^{-1}, but very similar R_H 52.2 ± 2.0 Pg C yr^{-1}. The comparison suggests that over the study period, the atmospheric aerosol loading enhanced the terrestrial ecosystem carbon uptake at the global scale, and slightly affected the autotrophic and heterotrophic respirations.

4.3. Spatial pattern of the aerosol effect on carbon dynamics

Over the study period 2003–2010, obvious positive aerosol effects on terrestrial ecosystem production (GPP, NPP and NEP) took place in vast areas in Central Africa, South and East Asia, reaching as large as 400 g C m^{-2} yr^{-1}. Slightly positive effects mainly happen in North America, Europe, northern coast area of Australia and Central South America. However, negative aerosol effects occurred in Amazonia region (especially the West Amazonia) and rainforest region in Indonesia Islands, as well as part of densely vegetated area in South China and Indochina.

The aerosol loading caused a 0.25 K decrease of the global annual average land surface temperature due to the reduction of solar energy received by the land surface (Fig. 4f). Further, aerosols affect soil physical properties by increasing 0.5% of the first-layer soil volumetric moisture content (Fig. 4g) and decreasing 0.71 K of the first-layer soil temperature (Fig. 4h). The spatial pattern of aerosol-caused differences of R_A is similar to the patterns of NPP because R_A is considered as a relatively constant proportion of the vegetation carbon gains (Gifford, 1994, 1995, 2003). However, while the differences of ecosystem production are high in East and Northeast China, the differences of R_A are not significant in these regions. The cooling effect of aerosol in these regions moderates the positive aerosol effect on R_A through the effect on GPP. In contrast, aerosol loadings result in less R_H in most areas of the globe except some regions in Central Africa, South and Southeast Asia and South America (Fig. 4e). Since soil temperature and soil moisture are positively correlated to the rate of R_H, the aerosol's positive effects on soil temperatures and negative effects on soil moisture mediate each other, and together determine the spatial pattern of the differences of R_H estimated by S0 and S1.

Aerosol has a positive effect on GPP, NPP and NEP for all the continents and the largest effect takes place in Africa (Fig. 5). However, the effect is with a high inter-annual variability in South America, showing that opposite effects happened in this continent. All continents show that aerosols enhanced R_A except Europe. R_H is negatively affected by aerosol in most continents but is slightly increased in Africa and Oceania.

5. Discussion

5.1. Aerosol effects associated with LAI and canopy structure

LAI has been recognised as one of the most important factors that exert direct or indirect influences on most land surface biophysical and biogeochemical processes (Bonan, 1993). Different from the other studies [e.g. Matsui et al., (2008)], we use prognostic rather than prescribed LAI (e.g. MODIS LAI). As a function of solar radiation, air temperature and humidity, LAI in the iTem, representing plant phenology of an ecosystem, therefore could be affected by the aerosol-induced changes of downward solar radiation (Stöckli et al., 2008, 2011). Our results show that aerosol causes LAI decrease in most regions where AOD are high, such as, in East Asia, Northern India, Amazonia forest area, Southeast United States and Europe (Fig. 6). However, aerosol loading increases LAI in vast area in Africa, South America and Australia, but with very small magnitudes. While the aerosol doesn't change the fraction of sunlit and shade LAI, which is purely determined by the solar zenith angle and leaf orientation distribution, it changes the magnitudes of sunlit and shaded LAI. The magnitude of sunlit LAI is slightly decreased over the most area of the globe because the aerosol reduces direct-beam solar radiation. The aerosol changed LAI in shaded leaves (Fig. 4c) and the spatial pattern of change of LAI_{sha} is very close to the change of total LAI.

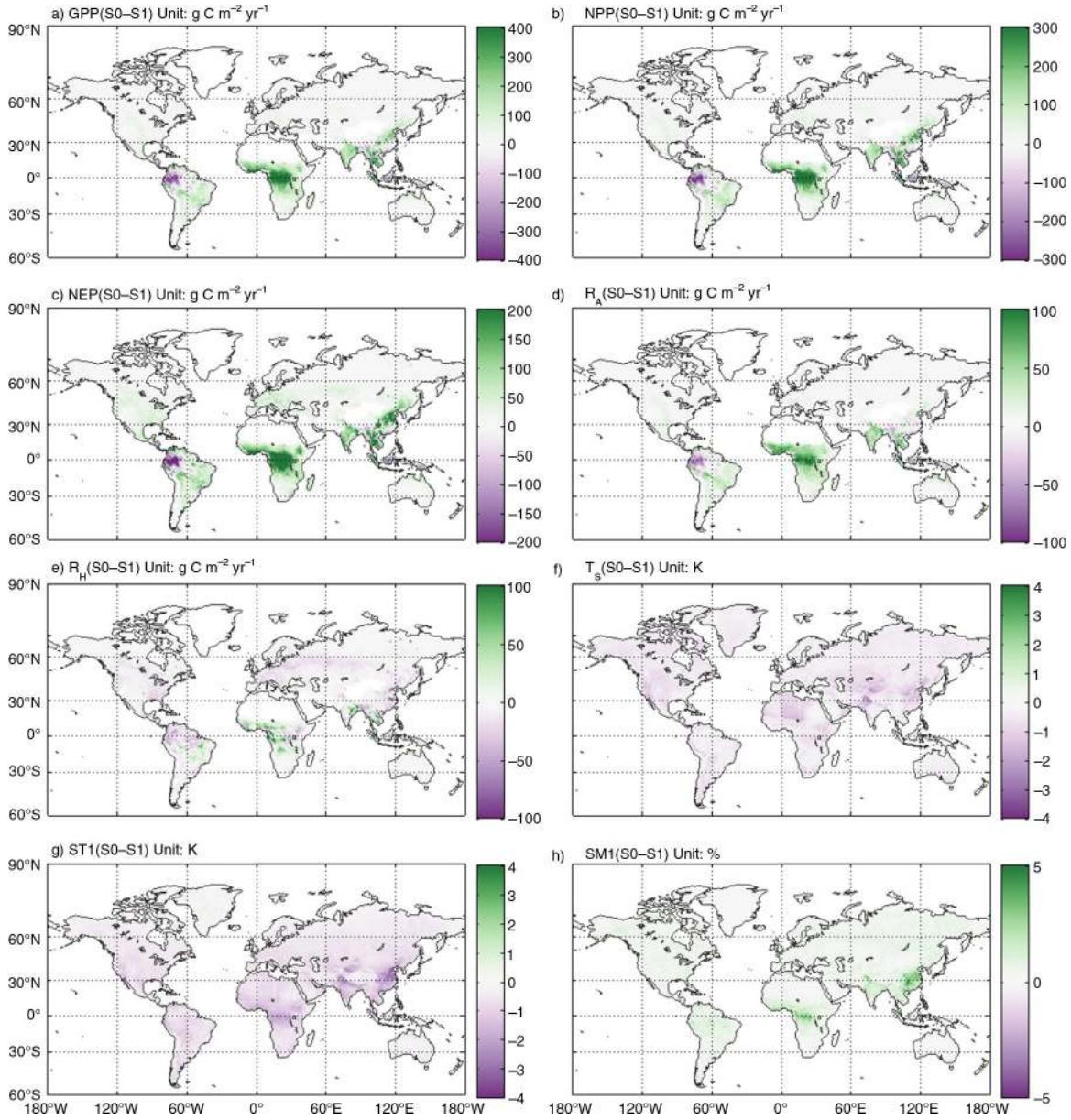

Fig. 4. Annually averaged differences of S0 and S1 carbon fluxes and land surface environmental variables over the period of 2003–2010. T_S is the land surface temperature; ST1 and SM1 are the first soil layer temperature and volumetric moisture content, respectively.

The aerosol effects on terrestrial ecosystem carbon dynamics are highly dependent on canopy LAI as previous studies suggested (Niyogi et al., 2004; Matsui et al., 2008). The positive relationship of LAI and the aerosol effects on the global ecosystem carbon uptakes (Fig. 7a, b, c) suggests that the aerosol effect is stronger for high-LAI ecosystems because of the increase of the proportion of the shaded leaves (Gu et al., 2003), which generally come with higher light-use efficiency comparing to sunlit leaves. Although aerosol loadings decrease land surface temperature (T_S), the impact is smaller with higher LAI (Fig. 7f). The impact of aerosol on R_A is positively correlated to LAI (Fig. 7d), which can be explained by the similar relationships of vegetation production and T_S. Overall the aerosol effect on soil temperature is negative (Fig. 7g), but the effect on soil moisture is positive (Fig. 7h) with LAI. They together result in the complex aerosol effect on R_H (Fig. 7e).

Different plant functional types have distinct responses to aerosols (Fig. 8). The tropical forest stands out to have the strongest positive response with 56.5 g C m^{-2} yr^{-1} increase of NEP. The magnitude of aerosol effect on xeric woodlands and temperate forests is after one of the tropical forest,

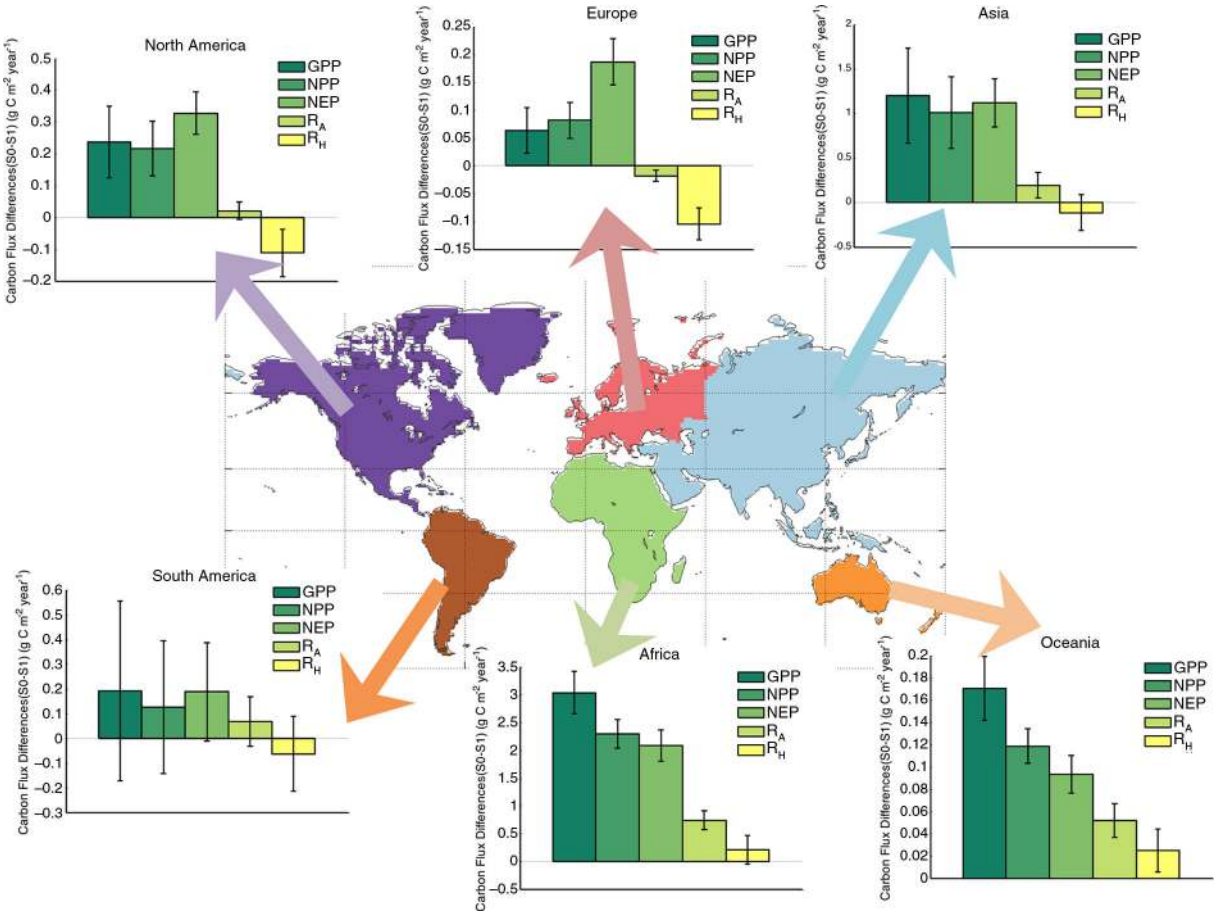

Fig. 5. Differences of the continent-based carbon fluxes over the study period. Error bars denote the standard deviation for the 8-yr values.

suggesting that the aerosol loading enhances 29.4–41.9 g m^{-2} C yr^{-1} net carbon uptake. Ecosystem production in middle- and low-latitudes are also enhanced by aerosol loadings (Fig. 8a, b, c). Although aerosol loading results in a positive response of boreal forest NEP, the aerosol caused a significant decrease of R_H, which compensates the negative effect of aerosols on plant carbon uptake (Fig. 8e). Aerosol inhibits the R_H for most PFTs because of its cooling effect (Fig. 8f, h), but the aerosol effect on soil moisture may moderate and even overwhelm the thermal effects on enhancing R_H in tropical forest and grassland with high inter-annual variability. Aerosol effects on R_A for each PFT are generally similar to the effects on GPP, but with smaller magnitudes. Forests generally have higher LAI (Fig. 9). Generally, grassland in tropical Africa has higher LAI than boreal forest. LAI varies little within the similar landscape class across the globe. For example, average LAI of temperature coniferous forest and temperate deciduous forest are close to each other. LAI alone cannot explain the distinct response of PFTs to aerosol effects (Figs. 8 and 9). The PFT specific canopy structure and physiological functioning as well as the environmental conditions may act together with LAI to determine the degree of the aerosol effect on carbon cycling. Overall, aerosols have a stronger effect on forest ecosystems. In addition, there are stronger effects on lower-latitude ecosystems (e.g. tropical forest) than that in higher latitudes (e.g. wet tundra). Most positive effects on ecosystem carbon gain happen in low-latitude areas, but negative effects exist widely in high-latitude ecosystems. These findings are consistent with previous studies (Gu et al., 2003; Krakauer and Randerson, 2003; Oliveira et al., 2007).

5.2. *Sunlit versus shaded leaves*

It is necessary to separate the canopy into sunlit and shaded parts to investigate the aerosol effect on terrestrial ecosystem carbon dynamics in detail since the two parts of canopy leaves respond differently to the change of radiation regime caused by aerosols (Wang and Leuning, 1998; Dai et al., 2004). While the aerosol-induced decrease of direct solar radiation might not affect photosynthesis of sunlit leaves

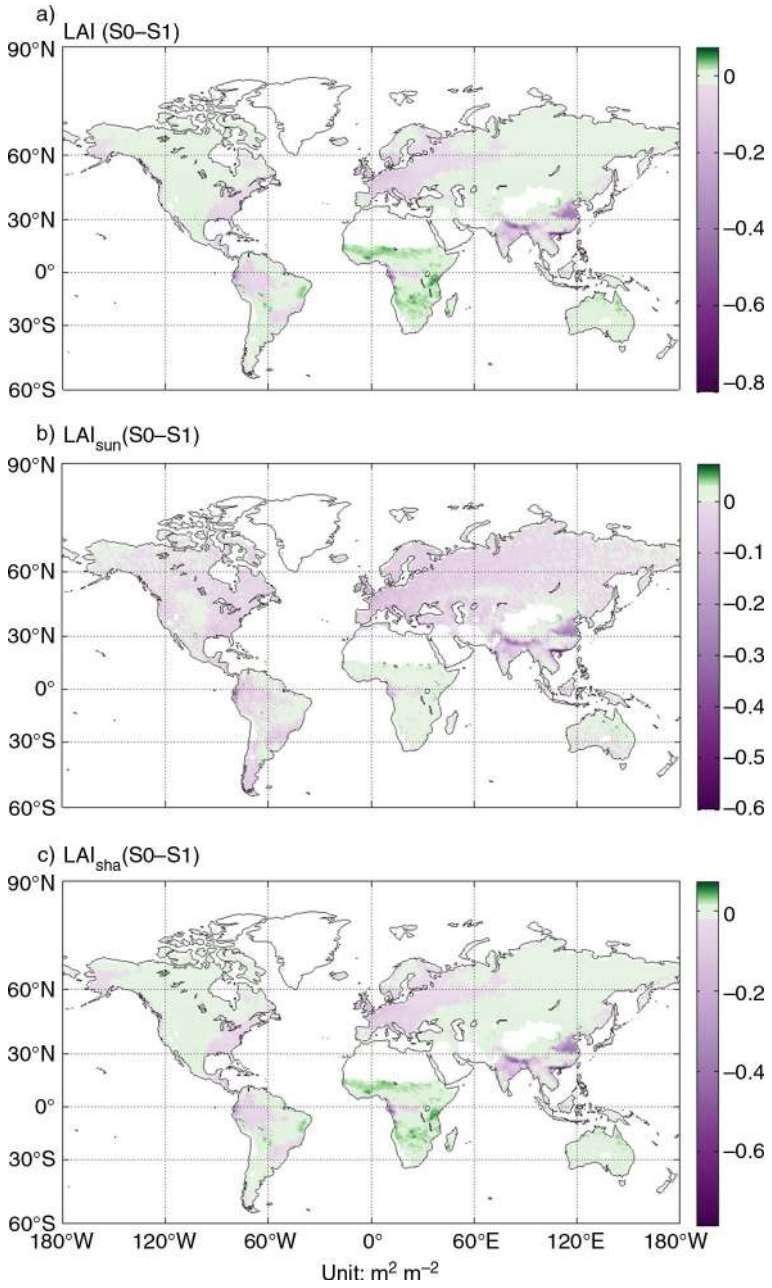

Fig. 6. Aerosol-caused changes of annual average global leaf area index.

because they are normally light-saturated, the enhancement of diffuse radiation could stimulate photosynthesis in shaded leaves. However, it is not necessarily true that aerosol always enhances diffuse solar radiation according to our calculation. For instance, the diffuse PAR is decreased over the Amazonia forest area due to aerosol radiative effects (Fig. 2) because of the much stronger scatter ability of clouds. Our results indeed show that the aerosol loading increases the amount of global carbon assimilation over the study period. The leaf-scale Rubisco-limited photosynthesis rate (J_C) and RuBP regeneration-limited (i.e. light-limited) photosynthesis rate (J_E) are shown geographically for both sunlit and shaded canopy photosynthesis (Fig. 10). In iTem, J_C is modelled to be directly limited by environmental factors including leaf temperature, plant nutrient supply and soil water content; J_E is estimated depending on the plant growing temperature, i.e. the average ambient temperature over the canopy during the preceding month, and PAR. Therefore J_E can be directly influenced by the aerosol light-scattering effect, while J_C could be indirectly affected by the

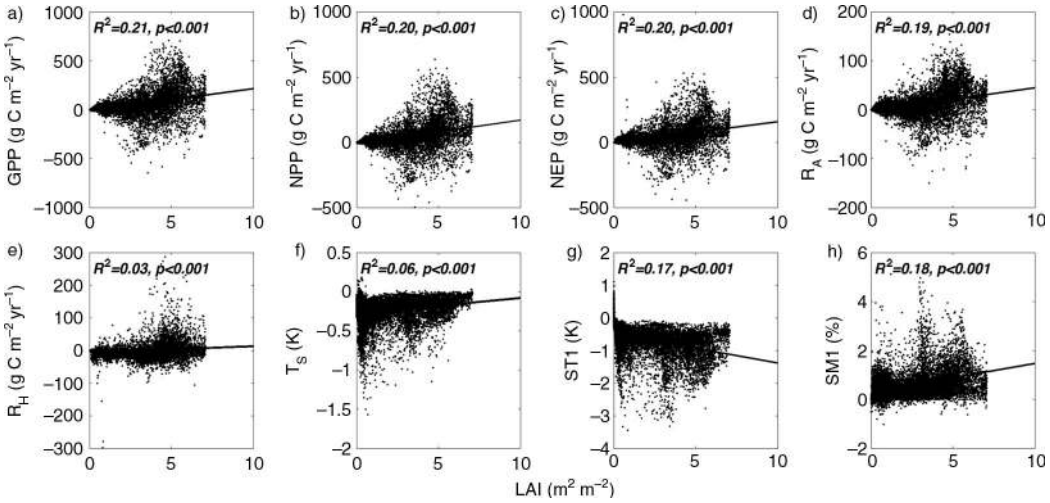

Fig. 7. Aerosol-induced changes of carbon fluxes and environmental variables at different leaf area index levels. The change is the difference between annual mean values of these variables of the S0 and S1 estimates.

variation of thermal and hydrologic conditions caused by the land surface radiation regime change. The actual leaf-scale photosynthesis rate is then limited by the minimum of these two rates (See descriptions of iTem in Chen, 2013).

For sunlit leaves, aerosol generally caused an increase of J_C in all the vegetated area because of the moderate of leaf temperature and the increased soil moisture (Fig. 4f, h and 10a). J_E in sunlit leaves are decreased because of the reduced

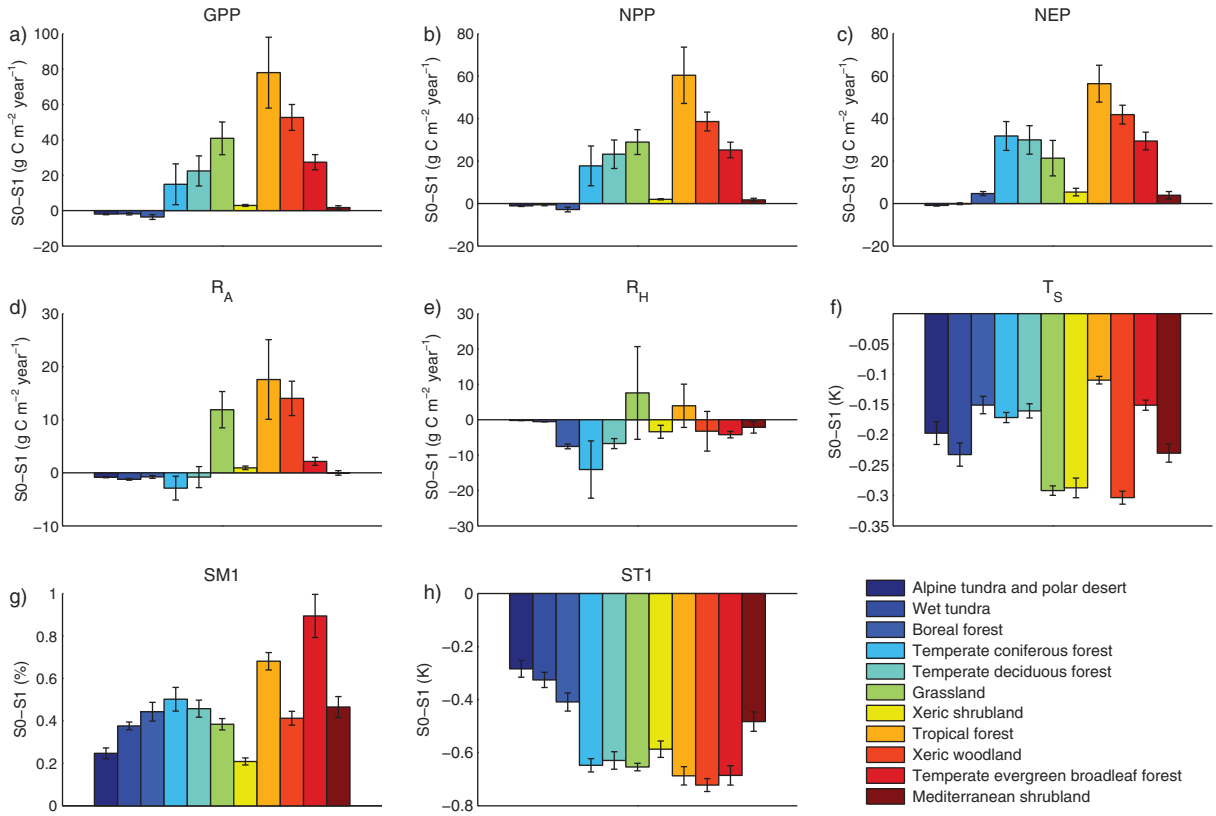

Fig. 8. Differences of plant functional type based carbon fluxes and environmental conditions over the study period. Error bars represent the standard deviation for the 8-yr values. T_S is the land surface temperature; ST1 and SM1 are the first soil layer temperature and volumetric moisture content, respectively.

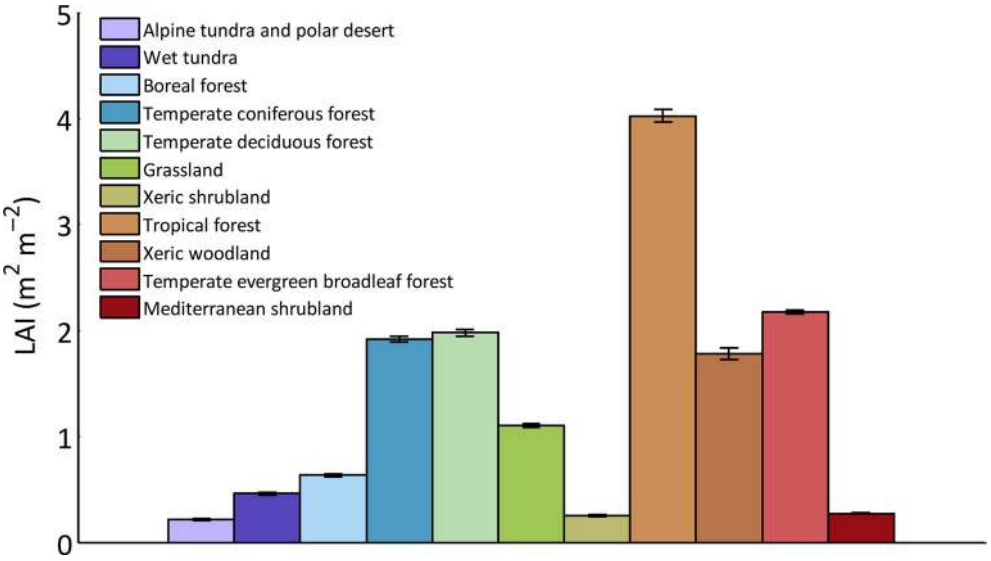

Fig. 9. Annual average leaf area index for each plant functional type of the S0 simulation. Error bars represent the standard deviation for the 8-yr values.

direct-beam PAR. For shaded leaves, J_C are also increased; however, the aerosol causes decrease of J_E in shade leaves in most of the dense vegetated area such as the tropical forests in Amazon and central Africa and the temperate forests in eastern China and United States (Fig. 10d); and the spatial pattern of the change of J_E is highly correlated to the change of diffuse PAR (Fig. 2). Our results indicate that photosynthesis in sunlit leaves are often light-saturated (i.e. $J_{C,sun}-J_{E,sun}<0$), but it is opposite in shaded leaves for the densely vegetated area (Fig. 10e, f). An outstanding exception happens in the tropical forests in the Amazonian area and the Indonesia Islands, where $J_{C,sha}$ and $J_{C,sun}$ are both larger than $J_{E,sha}$ and $J_{E,sun}$, respectively, suggesting that photosynthesis in these regions is light-limited. As discussed in Section 4.1, this is mainly because of high CF and dense water vapour concentration (Fig. 3) over these regions, which causes relatively lower solar radiation in this area (Cohan et al., 2002). The aerosol loading further reduces both direct-beam and diffuse PAR in these regions (Fig. 2) rather than enhancing the diffuse PAR. Together with the possible small aerosol-induced LAI change, the canopy-scale photosynthesis decreases in both sunlit and shaded leaves (GPP_{sun} and GPP_{sha}) in these regions (Fig. 6).

5.3. Aerosol impacts on thermal and hydrological conditions

Evidence has shown that the leaf temperature can vary as high as several degrees throughout a day in sunlit and shaded leaves (Smith and Nobel, 1977). Aerosol loading can affect land surface thermal and hydrological conditions through its influences on surface radiation regime. According to this general hypothesis, because of the effect of reducing incoming solar radiation, aerosol cools land surface and soil, therefore inhibits surface water transpiration and keeps higher soil moisture. On a global scale, our results are generally consistent with these processes. The land surface and the soil are cooled by aerosol loading (Fig. 4f, g and 10i, j) and the soil moisture is higher under aerosol conditions (Fig. 4h). The simulated aerosol indirect thermal and hydrological effects on carbon dynamics through influencing the environmental conditions are summarised in Fig. 11, indicating that the aerosol-caused change of GPP and changes of T_S, ST1 and SM1 are correlated at the global scale.

Figure 12 shows the relationship of the aerosol effect on carbon cycle at different thermal (i.e. measured by T_{gcm}) and moisture [i.e. measured by Vapor Pressure Deficit (VPD)] conditions at the global scale. Unit change of aerosol reduces GPP at cool ($T_{gcm}<284$ K) and humid (VPD <4hPa, close to water-saturated) conditions, but stimulates carbon uptake in hotter and drier conditions. The change of aerosol affects R_H in more complicated ways: negative effects happen at extreme conditions (both cool or hot, and dry or moist), while positive effects happen at moderate conditions. These findings are consistent with the Arrhenius-type of relationships between carbon fluxes and the temperature and the moisture conditions. The aerosol light-scattering effect indirectly cools and keeps more water on the land surface, and causes the major carbon cycling processes (photosynthesis and soil decomposition) either closer to or farther from the optimum situations, and therefore results in the variable responses of the carbon fluxes to the changing environmental conditions.

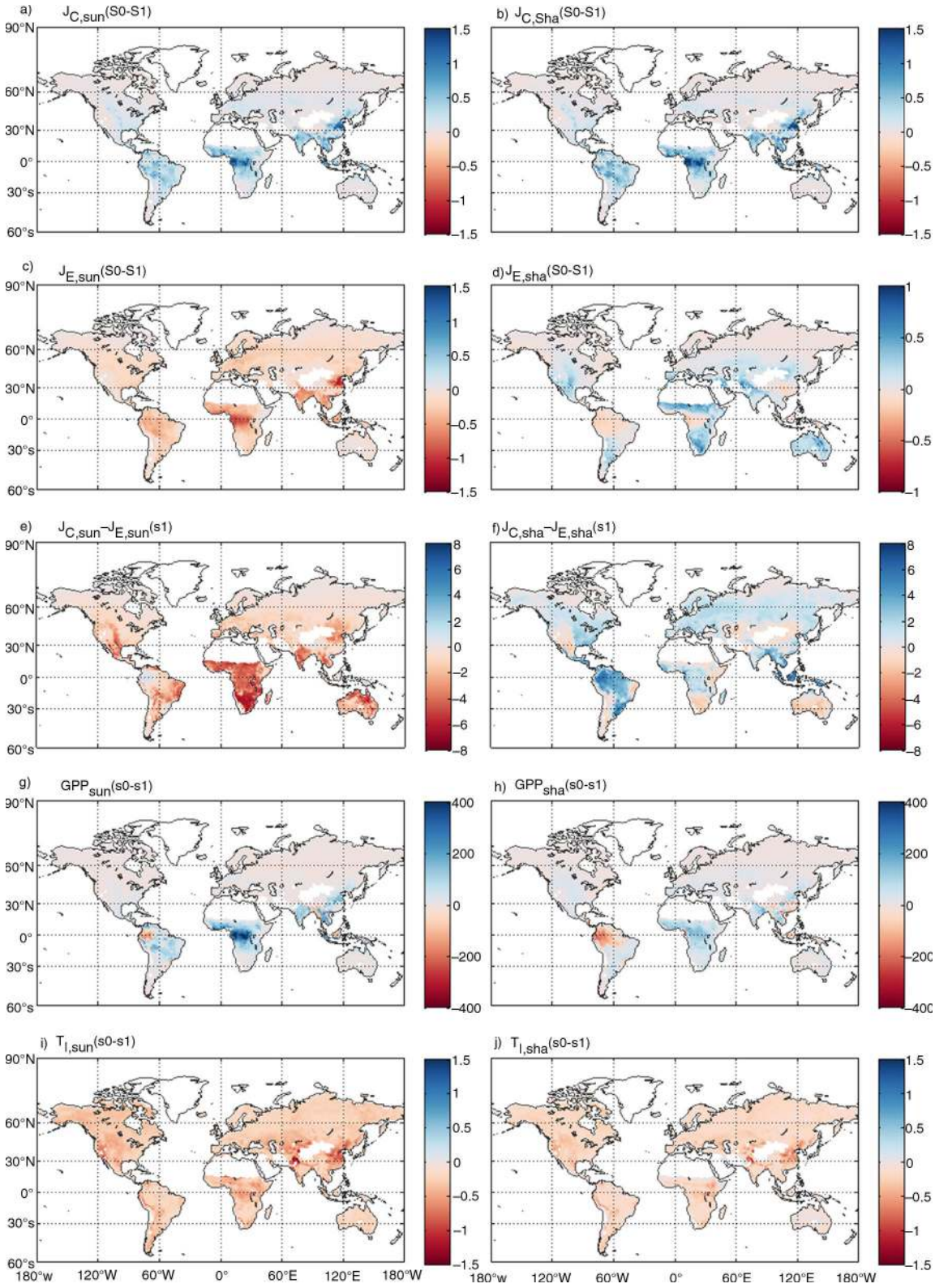

Fig. 10. Photosynthetic parameters for sunlit and shaded leaves. J_C and J_E: the leaf-scale Rubisco-limited photosynthesis rate and light-limited photosynthesis rate (Units: μmol CO_2 m^{-2} s^{-1}), respectively; GPP_{sun} and GPP_{sha}: canopy GPP (photosynthesis) for sunlit and shaded leaves (Units: g C m^{-2} yr^{-1}), respectively; T_l: annual average leaf temperature (Units: K).

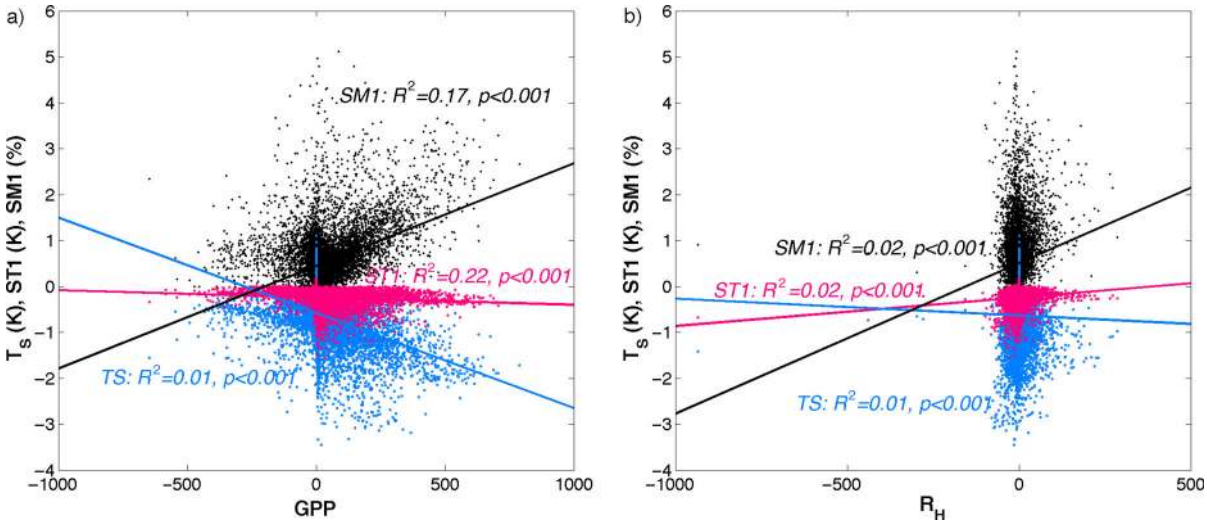

Fig. 11. Scatterplots of aerosol-induced changes of key carbon fluxes (GPP and R_H) and environmental conditions (T_S, ST1 and SM1). Units for the carbon fluxes are g C m^{-2} yr^{-1}.

The strong seasonal variations of aerosol effects on global carbon fluxes may further explain the aerosol thermal effect (Fig. 13). In the low-latitude (between 30°S and 30°N) area, the aerosol effect is mostly positive on GPP, NPP and NEP, and the strongest effect happens in the cool months (i.e. October, November, December and January for northern hemisphere, and May, June, July and August for southern hemisphere). The aerosol loading negatively affects the plant production in subtropical regions of the Northern Hemisphere (about 20°N) in summer months. In higher latitudes, the aerosol effect mainly happens in summer months, either positive (for Northern Hemisphere), or negative (for Southern Hemisphere). R_A has the similar seasonal pattern as the plant production. In higher-latitude area (above 30°), aerosol effects on R_H are negative and mainly happen in summer for both northern and southern hemispheres. R_H in tropical areas is negatively affected by aerosols in spring months and positively affected in other months. All the strongest effects happen under moderate to hot thermal conditions in which the cooling effect of aerosols may be significant in optimum thermal environments for carbon cycling.

5.4. *Limitations and future needs*

Aerosol direct radiative effects on terrestrial ecosystem carbon dynamics exist in various biophysical and biogeochemical processes. The modelling framework describing these processes may introduce uncertainties to the estimates. First, the MODIS measurement of the key atmospheric components has considerable errors (Levy et al., 2005; Li et al., 2012; Remer et al., 2005). In addition, the error of gap-filling the MODIS atmospheric products (Garcia, 2010; Wang et al., 2012) and the inaccuracy of the atmospheric radiative transfer model (Gueymard, 2008, 2012) may further contribute to the uncertainty of model estimates of aerosol effect on the amount of downward solar radiation and its partitioning. Second, uncertainties exist in the model structure and parameterisation of iTem. Although iTem has been carefully calibrated using observed data and its estimation of carbon fluxes show a good agreement with other results, there is always uncertainty associated with model parameterisation to some degree (Tang and Zhuang, 2008; Keenan et al., 2012). There are more factors that may influence the aerosol effect on carbon dynamics, but not considered in iTem, such as, a better representation of radiation transfer in the canopy (Bonan et al., 2011; Widlowski et al., 2011), dynamic vegetation (Sitch et al., 2003), and nitrogen deposition (Reay et al., 2008). Considering the importance of LAI in terrestrial ecosystem carbon cycling, the estimation of LAI in iTem may need to be improved in the future using better algorithms of leaf carbon allocation (Litton et al., 2007).

In this study, model simulations were conducted with different solar radiation regimes but with the same meteorological drivers (e.g. air temperature, relative humidity, etc.). While we recognise the importance of aerosol indirect effects on the land surface micrometeorology, the aerosol indirect effect, i.e. the aerosol can change the weather and climate (Ramanathan et al., 2001; Hansen et al., 2005; Rosenfeld et al., 2008), however, is not yet considered. Besides the effects caused by aerosol-reduced solar radiation, aerosol-enhanced diffuse radiation has also been found to be related to the change of air temperature

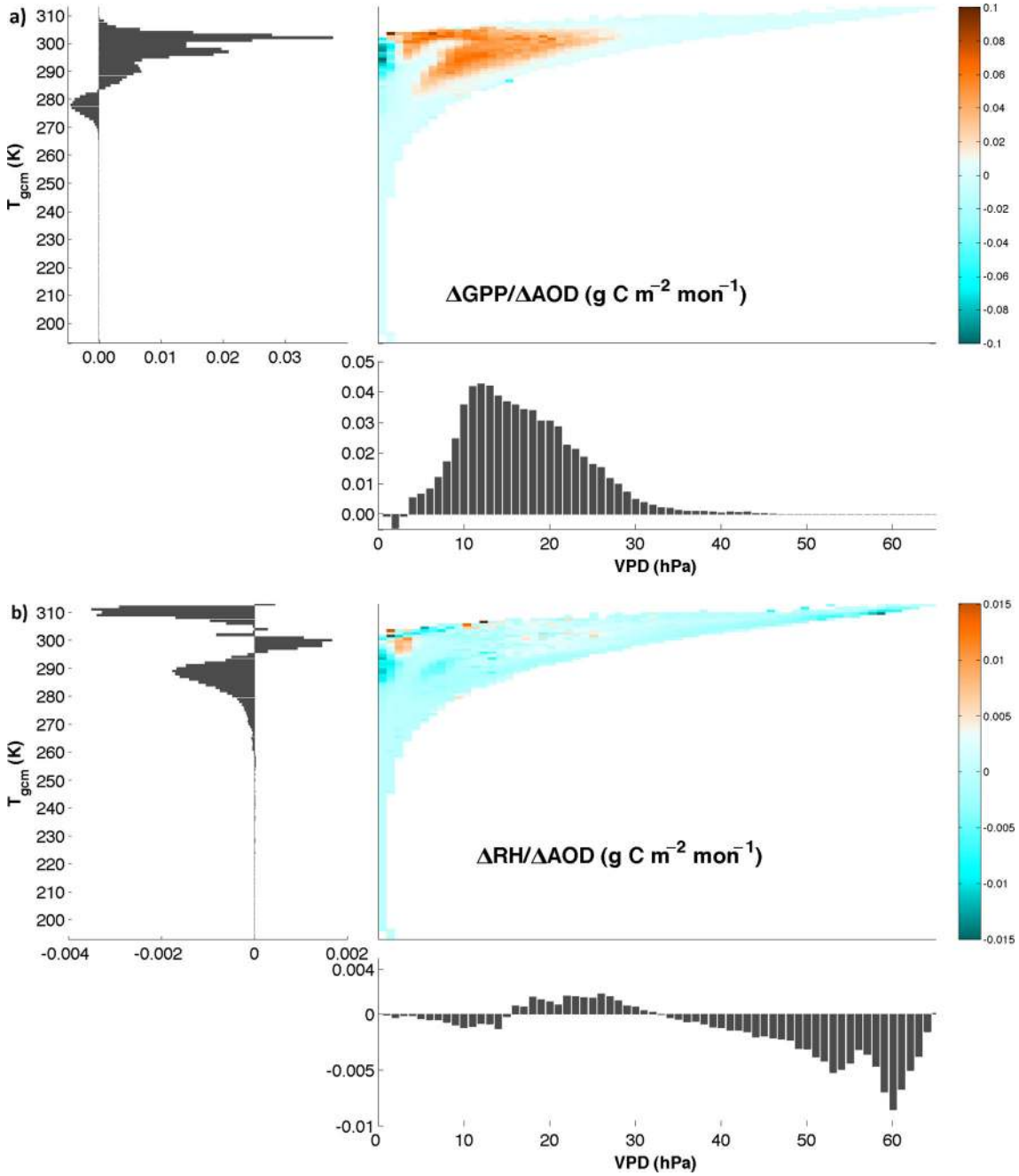

Fig. 12. Sensitivity of monthly averaged key carbon fluxes (GPP and RH) to unit change of AOD at different thermal and humid conditions. The units of the sensitivity of both the scatterplot and bar plots are g C mon^{-1}.

and VPD in terrestrial ecosystems (Gu et al., 2002). These aerosol indirect effects are not included in our study, but indeed they can considerably influence the ecosystem carbon dynamics. To include these indirect effects, the role of aerosol in the atmospheric circulation needs to be well understood and substantial efforts of fully coupled online atmosphere–ecosystem simulations should be conducted in the future. These online simulations, configured with more processes and interactions, may alter various conclusions made in this study.

The role of cloud has to be emphasised while evaluating the aerosol effect on terrestrial ecosystems. As stated in our study, the cloudiness is particularly critical to determining the aerosol effect since cloud's scattering effect is much stronger and can overwhelm the radiative effect of aerosol. Our results show that the parameter CF matters the most

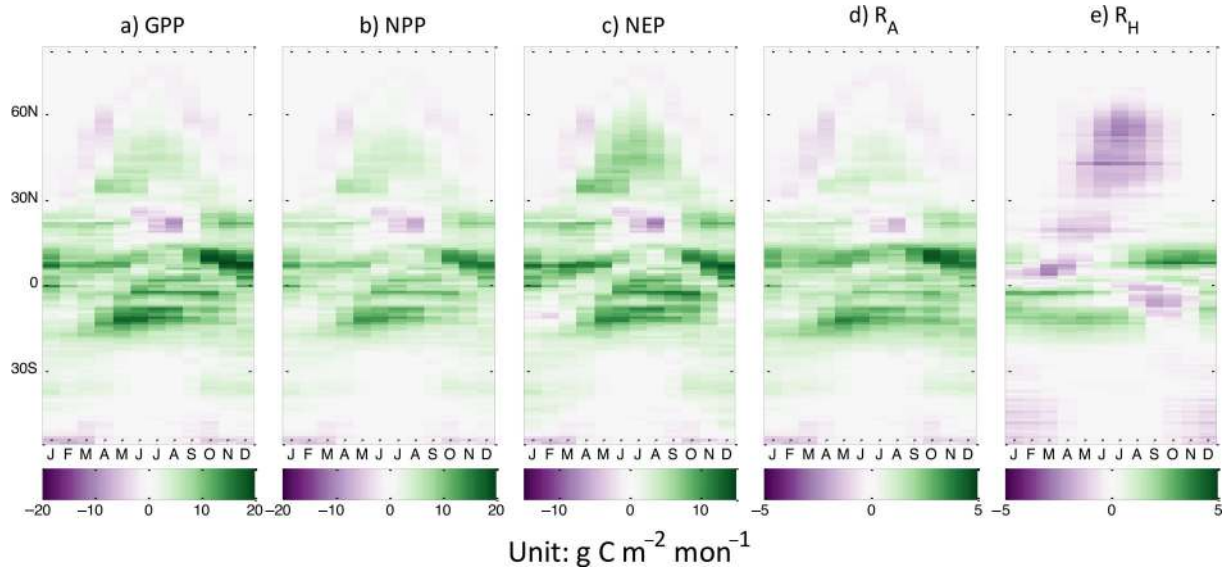

Fig. 13. Zonal mean differences between carbon fluxes (calculated as S0–S1) averaged over the study period.

to the spatial pattern of solar radiation received by land surface. Determination of which the limiting photosynthesis rate (i.e. J_C or J_E) is for both sunlit and shaded leaves highly depends on the solar radiation intensity that the leaves absorbed, which is mostly influenced by cloud (Fig. 10). Aerosol could act as cloud condensation nuclei, change the cloud droplet size distribution and change the cloud albedo (Twomey, 1977; Costantino and Bréon, 2010). Since clouds have strong effects on influencing solar radiation, this aerosol effect is referred to the aerosol indirect radiative effect. Clouds have been considered to have strong effects on ecosystem carbon uptake (Gu et al., 1999), therefore this aerosol indirect radiative effect couldn't be neglected for a full investigation of the aerosol radiative effects. Mercado et al. (2009) considered this indirect radiative effect together with the aerosol direct radiative effect by simply assuming an absolute reduction in below-cloud PAR equal to the absolute reduction in clear-sky PAR due to aerosols. However, the aerosol–cloud interactions are more complicated than the simple relationship suggested and remain a challenge in this field of research (Spichtinger and Daniel, 2008). Here our study is focusing on evaluating the aerosol direct radiative effect. Going forward, further work is needed to investigate both direct and indirect aerosol radiative effects.

6. Conclusion

Atmospheric aerosol has been considered to be able to considerably affect biogeochemistry and therefore climate change. One important aspect of aerosol effects is its impact on global carbon cycling. This study examines the aerosol influences on carbon dynamics of global terrestrial ecosystems through its light-scattering effect. Solar radiation estimated with and without consideration of aerosol is used to drive the iTem to analyse the ecosystem responses to different radiation regimes. We find that the aerosol light-scattering effect changed the carbon budget of the global terrestrial ecosystems during 2003–2010. The aerosol loading enhances both photosynthesis and plant autotrophic respiration, but moderately decreases heterotrophic respiration. Overall the global NPP and NEP are enhanced by aerosol. We found that aerosol also affects plant LAI, surface thermal and moist conditions, which indirectly affect carbon dynamics. Aerosol effects appear strongest in low-latitude and high LAI regions and in the seasons with moderate to hot thermal conditions. Our results suggest that the aerosol light-scattering effect should be considered in quantifying terrestrial ecosystem carbon dynamics and their feedbacks to the global climate system in the future.

7. Acknowledgements

We are very grateful to the editor and two anonymous reviewers for their constructive comments that helped us to improve this paper. This study is supported through a project (EAR-0630319) of NSF Carbon and Water in the Earth Program, a CDI-Type II project (IIS-1028291), NASA Land Use and Land Cover Change program with a project (NASA-NNX09AI26G), and a Department of Energy project (DE-FG02-08ER64599). The computing is supported by Rosen Center of high performance computing at Purdue.

References

Bonan, G. B. 1993. Importance of leaf area index and forest type when estimating photosynthesis in boreal forests. *Rem. Sens. Environ*. **43**, 303–314.

Bonan, G. B. 1996. *A Land Surface Model (LSM Version 1.0) for Ecological, Hydrological, and Atmospheric Studies: Technical Description and User's Guide*. NCAR Tech. Note, pp. 1–150.

Bonan, G. B., Lawrence, P. J., Oleson, K. W., Levis, S., Jung, M. and co-authors. 2011. Improving canopy processes in the Community Land Model version 4 (CLM4) using global flux fields empirically inferred from FLUXNET data. *J. Geophys. Res. Biogeosci*. **116**, G02014.

Chen, M. 2013. *Evaluation of Atmospheric Aerosol and Tropospheric Ozone Effects on Global Terrestrial Ecosystem Carbon Dynamics*. Doctor of Philosophy Department, Purdue University. Proquest Digital Dissertations.

Chen, M. and Zhuang, Q. 2012. Spatially explicit parameterization of a terrestrial ecosystem model and its application to the quantification of carbon dynamics of forest ecosystems in the conterminous United States. *Earth Interact*. **16**, 1–22.

Chen, M. and Zhuang, Q. 2013. Modeling temperature acclimation effects on carbon dynamics of forest ecosystems in the conterminous United States. *Tellus B*. **65,** 19156. doi: 10.3402/tellusb.v65i0.19156.

Chen, M., Zhuang, Q., Cook, D. R., Coulter, R., Pekour, M. and co-authors. 2011. Quantification of terrestrial ecosystem carbon dynamics in the conterminous United States combining a process-based biogeochemical model and MODIS and AmeriFlux data. *Biogeosciences*. **8**, 2665–2688.

Cohan, D. S., Xu, J., Greenwald, R., Bergin, M. H. and Chameides, W. L. 2002. Impact of atmospheric aerosol light scattering and absorption on terrestrial net primary productivity. *Glob. Biogeochem. Cycles*. **16**, 37-1–37-12.

Costantino, L. and Bréon, F.-M. 2010. Analysis of aerosol–cloud interaction from multi-sensor satellite observations. *Geophys. Res. Lett*. **37**, L11801.

Cramer, W., Kicklighter, D., Bondeau, A., Moore Iii, B., Churkina, G. and co-authors. 1999. Comparing global models of terrestrial net primary productivity (NPP): overview and key results. *Glob. Change Biol*. **5**, 1–15.

Dai, Y., Dickinson, R. E. and Wang, Y.-P. 2004. A two-big-leaf model for canopy temperature, photosynthesis, and stomatal conductance. *J. Clim*. **17**, 2281–2299.

FAO/UNESCO Soil map of the World (1:5 000 000), 1971–1981. FAO.

Garcia, D. 2010. Robust smoothing of gridded data in one and higher dimensions with missing values. *Comput. Stat. Data Anal*. **54**, 1167–1178.

Garcia, D. 2011. A fast all-in-one method for automated post-processing of PIV data. *Exp. Fluid*. **50**, 1247–1259.

Gifford, R. 1994. The global carbon cycle: a viewpoint on the missing sink. *Aust. J. Plant Physiol*. **21**, 1–15.

Gifford, R. 1995. Whole plant respiration and photosynthesis of wheat under increased CO_2 concentration and temperature: long-term vs. short-term distinctions for modelling. *Glob. Change Biol*. **1**, 385–396.

Gifford, R. 2003. Plant respiration in productivity models: conceptualisation, representation and issues for global terrestrial carbon-cycle research. *Funct. Plant Biol*. **30**, 171–186.

Gu, L., Baldocchi, D., Verma, S., Black, T., Vesala, T. and co-authors. 2002. Advantages of diffuse radiation for terrestrial ecosystem productivity. *J. Geophys. Res. Atmos*. **107**, 2–1.

Gu, L., Baldocchi, D. D., Wofsy, S. C., Munger, J. W., Michalsky, J. J. and co-authors. 2003. Response of a deciduous forest to the Mount Pinatubo eruption: enhanced photosynthesis. *Science*. **299**, 2035–2038.

Gu, L., Fuentes, J. D., Shugart, H. H., Staebler, R. M. and Black, T. A. 1999. Responses of net ecosystem exchanges of carbon dioxide to changes in cloudiness: results from two North American deciduous forests. *J. Geophys. Res. Atmos*. **104**, 31421–31434.

Gueymard, C. A. 2008. REST2: high-performance solar radiation model for cloudless-sky irradiance, illuminance, and photosynthetically active radiation – validation with a benchmark dataset. *Sol. Energ*. **82**, 272–285.

Gueymard, C. A. 2012. Clear-sky irradiance predictions for solar resource mapping and large-scale applications: improved validation methodology and detailed performance analysis of 18 broadband radiative models. *Sol. Energ*. **86**, 2145–2169.

Hansen, J., Nazarenko, L., Ruedy, R., Sato, M., Willis, J. and co-authors. 2005. Earth's energy imbalance: confirmation and implications. *Science*. **308**, 1431–1435.

IPCC. 2000. Land use, land-use change and forestry. (eds. R. T. Watson, I. R. Noble, B. Bolin, N. H. Ravindranath, D. J. Verardo and co-editors), Cambridge University Press, Cambridge, UK, pp. 375.

Kalnay, E., Kanamitsu, M., Kistler, R., Collins, W., Deaven, D. and co-authors. 1996. The NCEP/NCAR 40-year reanalysis project. *Bull. Am. Meteorol. Soc*. **77**, 437–471.

Kattge, J. and Knorr, W. 2007. Temperature acclimation in a biochemical model of photosynthesis: a reanalysis of data from 36 species. *Plant Cell Environ*. **30**, 1176–1190.

Keenan, T. F., Davidson, E., Moffat, A. M., Munger, W. and Richardson, A. D. 2012. Using model-data fusion to interpret past trends, and quantify uncertainties in future projections, of terrestrial ecosystem carbon cycling, Glob. Chang. *Biol*. **18**, 2555–2569.

Kistler, R., Collins, W., Saha, S., White, G., Woollen, J. and co-authors. 2001. The NCEP–NCAR 50–year reanalysis: monthly means CD–ROM and documentation. *Bull. Am. Meteorol. Soc*. **82**, 247–267.

Krakauer, N. Y. and Randerson, J. T. 2003. Do volcanic eruptions enhance or diminish net primary production? Evidence from tree rings, Glob. Biogeochem. *Cycles*. **17**, 1118.

Levy, R. C., Remer, L. A., Martins, J. V., Kaufman, Y. J., Plana-Fattori, A. and co-authors. 2005. Evaluation of the MODIS aerosol retrievals over ocean and land during CLAMS. *J. Atmos. Sci*. **62**, 974–992.

Li, H., Liu, Q., Du, Y., Jiang, J. and Wang, H. 2012. Evaluation of MODIS and NCEP atmospheric products for land surface temperature retrieval from HJ-1B IRS thermal infrared data with ground measurements, 5057–5060. In: *Proceedings of the Geoscience and Remote Sensing Symposium (IGARSS), 2012 IEEE International*, Munich, Germany, 22–27 July 2012.

Liou, K. N. 2002. *An Introduction to Atmospheric Radiation*. Academic Press, California, USA.

Litton, C. M., Raich, J. W. and Ryan, M. G. 2007. Carbon allocation in forest ecosystems. *Glob. Chang. Biol.* **13**, 2089–2109.

Lu, X., Kicklighter, D. W., Melillo, J. M., Yang, P., Rosenzweig, B. and co-authors. 2013. A contemporary carbon balance for the northeast region of the United States. *Environ. Sci. Technol.* **47**, 13230–13238.

Lu, X. and Zhuang, Q. 2010. Evaluating climate impacts on carbon balance of the terrestrial ecosystems in the midwest of the United States with a process-based ecosystem model. *Mitig. Adapt. Strat Glob. Chang.* **15**, 467–487.

Mahowald, N., Lindsay, K., Rothenberg, D., Doney, S. C., Moore, J. K. and co-authors. 2011a. Desert dust and anthropogenic aerosol interactions in the Community Climate System Model coupled-carbon–climate model. *Biogeosciences.* **8**, 387–414.

Mahowald, N., Ward, D. S., Kloster, S., Flanner, M. G., Heald, C. L. and co-authors. 2011b. Aerosol impacts on climate and biogeochemistry. *Ann. Rev. Environ. Resour.* **36**, 45–74.

Matsui, T., Beltrán-Przekurat, A., Niyogi, D., Pielke, R. A., Sr. and Coughenour, M. 2008. Aerosol light scattering effect on terrestrial plant productivity and energy fluxes over the eastern United States. *J. Geophys. Res.* **113**, D14S14.

McGuire, A. D., Joyce, L. A., Kicklighter, D. W., Melillo, J. M., Esser, G. and co-authors. 1993. Productivity response of climax temperate forests to elevated temperature and carbon dioxide: a North American comparison between two global models. *Clim. Chang.* **24**, 287–310.

McGuire, A. D., Melillo, J. M., Joyce, L. A., Kicklighter, D. W., Grace, A. L. and co-authors. 1992. Interactions between carbon and nitrogen dynamics in estimating net primary productivity for potential vegetation in North America. *Glob. Biogeochem. Cycles.* **6**, 101–124.

Melillo, J. M., McGuire, A. D., Kicklighter, D. W., Moore, B., Vorosmarty, C. J. and co-authors. 1993. Global climate change and terrestrial net primary production. *Nature.* **363**, 234–240.

Mercado, L. M., Bellouin, N., Sitch, S., Boucher, O., Huntingford, C. and co-authors. 2009. Impact of changes in diffuse radiation on the global land carbon sink. *Nature.* **458**, 1014–1017.

Niyogi, D., Chang, H.-I., Saxena, V. K., Holt, T., Alapaty, K. and co-authors. 2004. Direct observations of the effects of aerosol loading on net ecosystem CO_2 exchanges over different landscapes. *Geophys. Res. Lett.* **31**, L20506.

Oliveira, P. H. F., Artaxo, P., Pires, C., De Lucca, S., ProcÓPio, A. and co-authors. 2007. The effects of biomass burning aerosols and clouds on the CO_2 flux in Amazonia. *Tellus B.* **59**, 338–349.

Raich, J. W., Rastetter, E. B., Melillo, J. M., Kicklighter, D. W., Steudler, P. A. and co-authors. 1991. Potential net primary productivity in South America: application of a global model. *Ecol. Appl.* **1**, 399–429.

Ramanathan, V., Crutzen, P. J., Kiehl, J. T. and Rosenfeld, D. 2001. Aerosols, climate, and the hydrological cycle. *Science.* **294**, 2119–2124.

Reay, D. S., Dentener, F., Smith, P., Grace, J. and Feely, R. A. 2008. Global nitrogen deposition and carbon sinks. *Nat. Geosci.* **1**, 430–437.

Remer, L. A., Kaufman, Y. J., Tanré, D., Mattoo, S., Chu, D. A. and co-authors. 2005. The MODIS aerosol algorithm, products, and validation. *J. Atmos. Sci.* **62**, 947–973.

Roderick, M., Farquhar, G., Berry, S. and Noble, I. 2001. On the direct effect of clouds and atmospheric particles on the productivity and structure of vegetation. *Oecologia.* **129**, 21–30.

Rosenfeld, D., Lohmann, U., Raga, G. B., O'Dowd, C. D., Kulmala, M. and co-authors. 2008. Flood or drought: how do aerosols affect precipitation? *Science.* **321**, 1309–1313.

Sheffield, J., Goteti, G. and Wood, E. F. 2006. Development of a 50-year high-resolution global dataset of meteorological forcings for land surface modeling. *J. Clim.* **19**, 3088–3111.

Shekar Reddy, M. and Venkataraman, C. 2000. Atmospheric optical and radiative effects of anthropogenic aerosol constituents from India. *Atmos. Environ.* **34**, 4511–4523.

Sitch, S., Smith, B., Prentice, I., Arneth, A., Bondeau, A. and co-authors. 2003. Evaluation of ecosystem dynamics, plant geography and terrestrial carbon cycling in the LPJ dynamic global vegetation model. *Glob. Chang. Biol.* **9**, 161–185.

Smith, W. K. and Nobel, P. S. 1977. Temperature and water relations for sun and shade leaves of a desert broadleaf, hyptis emoryi. *J. Exp. Bot.* **28**, 169–183.

Spichtinger, P. and Daniel, J. C. 2008. Aerosol–cloud interactions – a challenge for measurements and modeling at the cutting edge of cloud–climate interactions. *Environ. Res. Lett.* **3**, 025002.

Stephens, G. L., Ackerman, S. and Smith, E. A. 1984. A shortwave parameterization revised to improve cloud absorption. *J. Atmos. Sci.* **41**, 687–690.

Stöckli, R., Rutishauser, T., Baker, I., Liniger, M. A. and Denning, A. S. 2011. A global reanalysis of vegetation phenology. *J. Geophys. Res. Biogeosci.* **116**, G03020.

Stöckli, R., Rutishauser, T., Dragoni, D., O'Keefe, J., Thornton, P. E. and co-authors. 2008. Remote sensing data assimilation for a prognostic phenology model. *J. Geophys. Res. Biogeosci.* **113**, G04021.

Tang, J. and Zhuang, Q. 2008. Equifinality in parameterization of process-based biogeochemistry models: a significant uncertainty source to the estimation of regional carbon dynamics. *J. Geophys. Res.* **113**, G04010.

Twomey, S. 1977. The influence of pollution on the shortwave albedo of clouds. *J. Atmos. Sci.* **34**, 1149–1152.

Van Laake, P. E. and Sanchez-Azofeifa, G. A. 2005. Mapping PAR using MODIS atmosphere products. *Rem. Sens. Environ.* **94**, 554–563.

Wang, G., Garcia, D., Liu, Y., de Jeu, R. and Johannes Dolman, A. 2012. A three-dimensional gap filling method for large geophysical datasets: application to global satellite soil moisture observations. *Environ. Model. Software.* **30**, 139–142.

Wang, Y. P. and Leuning, R. 1998. A two-leaf model for canopy conductance, photosynthesis and partitioning of available energy I: model description and comparison with a multi-layered model. *Agr. Forest Meteorol.* **91**, 89–111.

Widlowski, J. L., Pinty, B., Clerici, M., Dai, Y., De Kauwe, M. and co-authors. 2011. RAMI4PILPS: an intercomparison of

formulations for the partitioning of solar radiation in land surface models. *J. Geophys. Res. Biogeosci.* **116**, G02019.

Yuan, W., Liu, S., Yu, G., Bonnefond, J.-M., Chen, J. and co-authors. 2010. Global estimates of evapotranspiration and gross primary production based on MODIS and global meteorology data. *Rem. Sens. Environ.* **114**, 1416–1431.

Zhuang, Q., McGuire, A. D., Melillo, J. M., Clein, J. S., Dargaville, R. J. and co-authors. 2003. Carbon cycling in extratropical terrestrial ecosystems of the Northern Hemisphere during the 20th century: a modeling analysis of the influences of soil thermal dynamics. *Tellus B.* **55**, 751–776.

Ziehn, T., Kattge, J., Knorr, W. and Scholze, M. 2011. Improving the predictability of global CO_2 assimilation rates under climate change. *Geophys. Res. Lett.* **38**, L10404.